# Characterisation of the conformational changes in platelet factor 4 induced by polyanions: towards *in vitro* prediction of antigenicity

**Sven Brandt[1]; Krystin Krauel[1,2]; Kay E. Gottschalk[3]; Thomas Renné[4,6]; Christiane A. Helm[5]; Andreas Greinacher[2*]; Stephan Block[1*]**

[1]ZIK HIKE – Zentrum für Innovationskompetenz „Humorale Immunreaktionen bei kardiovaskulären Erkrankungen", Greifswald, Germany; [2]Institut für Immunologie und Transfusionsmedizin, Greifswald, Germany; [3]Institut für Experimentelle Physik, Universität Ulm, Ulm, Germany; [4]Department of Molecular Medicine and Surgery, Karolinska Institutet, Stockholm, Sweden; [5]Institut für Physik, Ernst-Moritz-Arndt Universität, Greifswald, Germany; [6]Institute for Clinical Chemistry and Laboratory Medicine, University Hospital Hamburg-Eppendorf, Hamburg, Germany

## Summary

Heparin-induced thrombocytopenia (HIT) is the most frequent drug-induced immune reaction affecting blood cells. Its antigen is formed when the chemokine platelet factor 4 (PF4) complexes with polyanions. By assessing polyanions of varying length and degree of sulfation using immunoassay and circular dichroism (CD)-spectroscopy, we show that PF4 structural changes resulting in antiparallel β-sheet content >30% make PF4/polyanion complexes antigenic. Further, we found that polyphosphates (polyP-55) induce antigenic changes on PF4, whereas fondaparinux does not. We provide a model suggesting that conformational changes exposing antigens on PF4/polyanion complexes occur in the hairpin involving AA 32–38, which form together with C-terminal AA (66–70) of the adjacent PF4 monomer a continuous patch on the PF4 tetramer surface, explaining why only tetrameric PF4 molecules express "HIT antigens". The correlation of antibody binding in immunoassays with PF4 structural changes provides the intriguing possibility that CD-spectroscopy could become the first antibody-independent, *in vitro* method to predict potential immunogenicity of drugs. CD-spectroscopy could identify compounds during preclinical drug development that induce PF4 structural changes correlated with antigenicity. The clinical relevance can then be specifically addressed during clinical trials. Whether these findings can be transferred to other endogenous proteins requires further studies.

## Keywords

Heparin-induced thrombocytopenia, platelet factor 4, GAGs, CD spectroscopy, antigenicity

**Correspondence to:**
Prof. Dr. med. Andreas Greinacher
Institut für Immunologie und Transfusionsmedizin
Sauerbruchstrasse
17475 Greifswald, Germany
Tel.: +49 3834 865482, Fax: +49 3834 865489
E-mail: greinach@uni-greifswald.de
or
Stephan Block, PhD
Applied Physics, Chalmers University of Technology
Fysikgränd 3, S-412 96 Gothenburg, Sweden;
E-mail: block@physik.uni-greifswald.de, stephan.block@chalmers.se

Received: August 2, 2013
Accepted after major revision: January 20, 2014
Prepublished online: March 27, 2014

**http://dx.doi.org/10.1160/TH13-08-0634**
**Thromb Haemost 2014; 112: ■■■**

* Shared senior authorship.

## Introduction

One of the major challenges for the development of new biotherapeutics is their potential immunogenicity (1, 2). Several drugs have failed when immune-mediated adverse effects became only obvious during phase III clinical trials (3, 4). Immunogenicity can be caused by the drug itself as a foreign protein as shown by recombinant hirudin (a leech derived protein) (5, 6), by conformational changes of endogenous proteins (induced during manufacturing or storing processes) as shown for erythropoietin (7), or by clustering of the protein as shown for interferon β (8, 9).

Currently, the most frequent immune-mediated adverse drug effect affecting blood cells is induced by the anticoagulant heparin (10). Polyanions (PAs) like heparin bind to the positively charged chemokine platelet factor 4 (PF4; CXCL4) (11–15) forming large complexes that are highly immunogenic (16, 17). The resulting immunoglobulin G (IgG) antibodies can then trigger the adverse drug effect heparin-induced thrombocytopenia (HIT) (10, 18–22).

Although HIT has been actively studied for several decades, relatively little is known about the molecular mechanisms leading to the formation of antigenic structures to which the anti-PF4/heparin antibodies bind (23). As heparin can be replaced by other PAs without changing the antigenicity of the resulting PF4/PA complexes (23–25), it is widely accepted that the immunogenic epitopes are located on PF4. NMR measurements suggest that complex antigenicity is accompanied by structural changes of PF4 (27); however, there is no direct experimental proof for PA-induced changes in the secondary structure of PF4. Recently we observed by circular dichroism (CD) spectroscopy that PF4 undergoes a structural change if bound to certain PAs. Most interestingly, nucleic acid constructs that induced a conformational change of PF4 also induced anti-PF4/PA antibodies *in vivo* (26).

In this study, we now systematically characterise the structural changes of PF4 induced by binding to various PAs using CD spectroscopy and correlate these changes with the exposure of antigenic epitope(s) on PF4, i.e. allowing binding of anti-PF4/polyanion antibodies. We show that CD spectroscopy provides a potential *in vitro* tool to predict the potential of a PA to induce antigenic epitopes on PF4 and provide a model on the antigenic sites on PF4.

## Materials and methods

Proteins and chemicals used were: Lyophilised, human platelet factor 4 (PF4) was isolated from platelets (Chromatec, Greifswald, Germany). Polyanions (PA): unfractioned heparin (UFH; Ratiopharm GmbH, Ulm, Germany), 2-O, 3-O desulfated heparin (ODSH; ParinGenix Inc., Weston, FL USA), reviparin (Clivarin 1750, Abbott GmbH & Co KG, Wiesbaden, Germany), fondaparinux (Arixtra 2.5 mg/0.5 mL, GlaxoSmithKline, Durham, NC, USA); hyaluronic acid, dextran sulfate; chondroitin sulfate A (Sigma-Aldrich, Munich, Germany) and polyphosphates of mean chain length 55 (polyP55; ICL Business Unit Bekaphos, Ladenburg, Germany).

### Circular dichroism (CD) spectroscopy

Changes in the secondary structure of PF4 upon interaction with PAs were studied by recording far-UV CD spectra (200–260 nm) using a Chirascan CD spectrometer (Applied Photophysics, Leatherhead, UK). PF4 was dissolved in phosphate-buffered saline (PBS; pH 7.2; Invitrogen, Darmstadt, Germany) to final concentrations of 40 µg/ml (1.25 µmol/l) or 80 µg/ml (2.5 µmol/l). Complex formation was carried out at 20°C directly within the CD cuvette (Hellma, Müllheim, Germany). Each measurement started with a pure PF4 solution whose initial concentration was set to 40 µg/ml (cuvette path length = 10 mm) or 80 µg/ml (cuvette path length = 5 mm). Afterward, increasing amounts of a certain PA were sequentially added to the cuvette (leading to defined PF4/PA mixtures) and a CD spectrum was recorded for each mixing step. Additionally, buffer baselines, baselines of each PA concentration step (without PF4 in the solution) were recorded.

In the data analysis, the spectra of PF4 alone and of PF4/PA complexes were corrected for the baselines, path length, concentration, and number of amino acids to obtain the wavelength-dependent mean residue delta epsilon (MRDE) values of the PF4/PA complex. To estimate the secondary structure content of PF4, deconvolution of CD-spectra was carried out with CDNN (software, circular dichroism neural network) using a database of 33 reference proteins (28). In the deconvolution process calculations were adjusted for the moderate dilution of PF4 (due to addition of the PA solution).

### Enzyme immunoassay (EIA)

PF4/PA EIA was performed with human sera of patients known to contain anti-PF4/heparin IgG verified by PF4/heparin EIA and heparin-induced platelet activation (HIPA) test as described (29) with some modifications. PF4 (20 µg/ml) was incubated (60 minutes [min] at room temperature [RT]) with rising concentrations of the PAs (as indicated in the figures) in coating buffer (0.05 M $NaH_2PO_4$, 0.1% $NaN_3$) to enable complex formation before coating wells of a microtiter plate (CovaLink, Nunc, Langenselbold, Germany) with 100 µl at 4°C overnight. Then plates were washed five times (0.15 M NaCl, 0.1% Tween 20, pH 7.5) and incubated (60 min, RT) with 100 µl patient serum (1:200 or 1:1,000 in 0.05 M $NaH_2PO_4$, 0.15 M NaCl, 7.5% goat normal serum, pH 7.5). Plates were washed five times and incubated with 100 µl peroxidase-conjugated anti-human IgG (1:20,000, Dianova, Hamburg, Germany). Afterward, plates were washed five times and incubated (10 min, RT) with 100 µl tetramethylbenzidine. The reaction was stopped with 100 µl 1 M $H_2SO_4$ and absorbance was measured at 450 nm.

### Ethics

The use of human sera containing anti-PF4/heparin antibodies and obtaining whole blood from healthy volunteers was approved by the Greifswald ethics board.

## Results

### Changes in PF4 secondary structure due to interaction with UFH

►Figure 1 summarises the CD spectroscopic measurements on PF4/UFH complexes with defined molar ratios of PF4 and UFH. The concentration of PF4 was 40 or 80 µg/ml, respectively ($1.25 \cdot 10^{-6}$ M or $2.5 \cdot 10^{-6}$ M), while the UFH concentration was stepwise increased from 0 to 107 µg/ml, which corresponds to a maximum UFH concentration of $0.35 \cdot 10^{-3}$ M (per saccharide monomer). During the titration process, pronounced changes in the CD spectra are observed (►Figure 1A, B): (i) For UFH concentrations increasing from 0 to 6.9 µg/ml ($2.2 \cdot 10^{-5}$ M per saccharide monomer) the whole spectrum shifts upward, i.e. toward lower absolute ellipticity values. (ii) For a further concentration increase, this trend reverses (►Figure 1B). Excess of UFH leads to folding of PF4 towards its native conformation (►Figure 1A, B).

The spectrum of native PF4 shows two negative bands at 205 nm and 220 nm whose absolute values correspond to the α-helix content of the protein (30). The intensity of these bands changes for different UFH concentrations, indicating alterations in the secondary structure of PF4. Deconvolution of the CD spectra shows that complex formation of PF4 with UFH decreases the α-helix and β-turn content, which is balanced by an increase in antiparallel β-sheet content (►Figure 1C). For the remaining types of secondary structure, only insignificant changes are observed. Maximal changes are found for a UFH concentration of 6.9 µg/ml (at a PF4 concentration of 40 µg/ml), which corresponds to a stoichio-

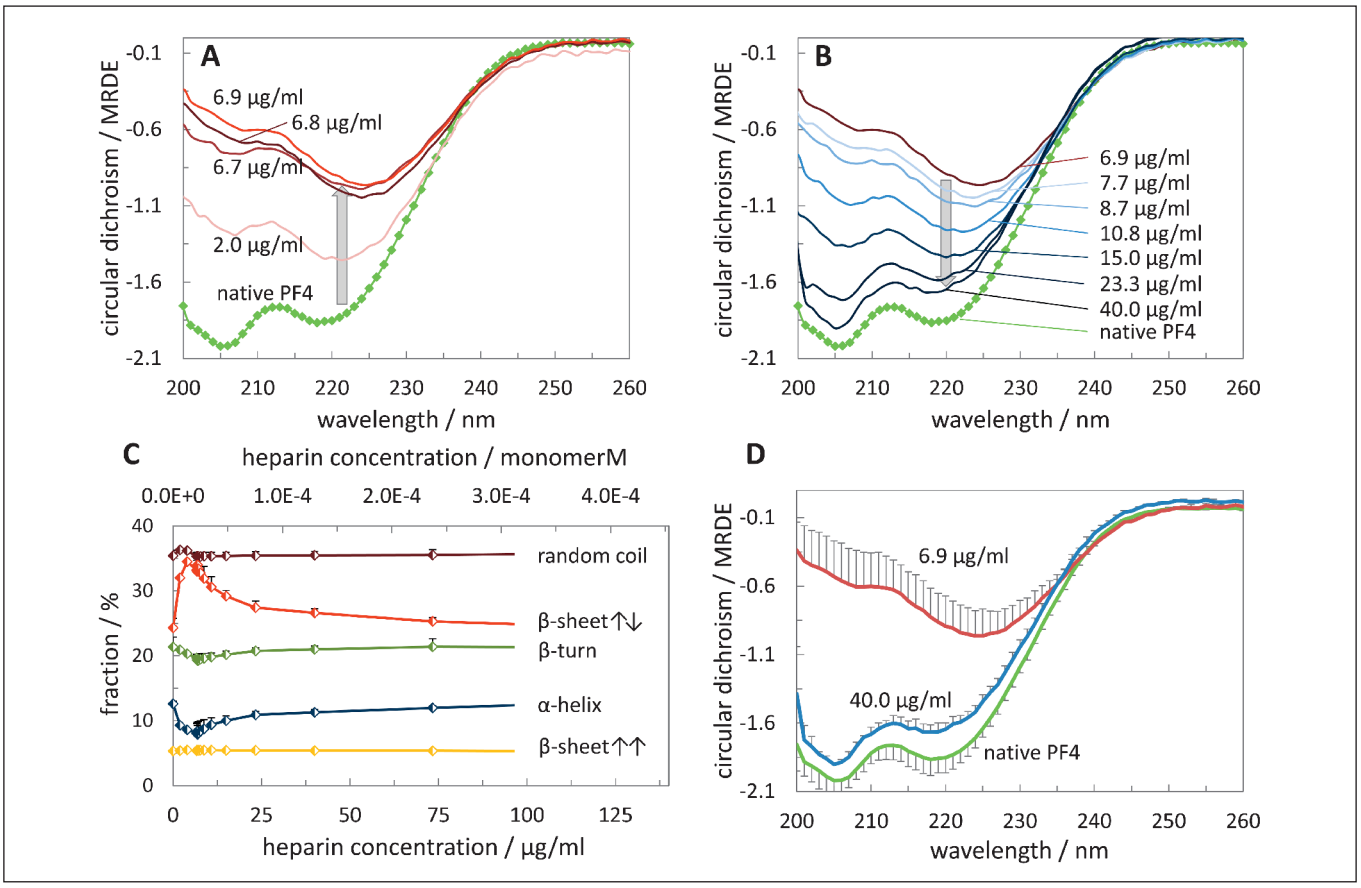


**Figure 1: Binding to unfractionated heparin (UFH) changes the secondary structure of platelet factor 4 (PF4).** CD spectra and secondary structure of PF4 in PF4/UFH complexes formed at various UFH concentrations as indicated (PF4 concentration = 40 µg/ml): A) – with increasing UFH concentration the CD spectra of PF4 shift to more positive ellipticity values, indicating changes in PF4 secondary structure, B) – with further increasing the UFH concentration, a return to a native-like state is observed, C) – deconvolution of the PF4/heparin CD spectra shows an increase in antiparallel β-sheet content (β-sheet ↑↓), which is balanced by a decrease in α-helix and β-turn content, D) – comparison of CD spectra of native PF4 (green) and of the PF4/UFH complex, formed at a concentration of 6.9 µg/ml (red) or in excess of UFH (native-like folding state; blue). The error bars correspond to the standard deviation, taken from the results of n = 3 experiments.

metric ratio of 18 saccharide monomers bound to one PF4 tetramer. Additionally, ▶Figure 1D shows that the CD spectrum of native PF4 and of the PF4/UFH complexes formed at 6.9 µg/ml and in excess of UFH = 40.0 µg/ml), albeit similar, still significantly differ from each other.

## Correlation of PF4 structural changes and PF4/PA complex antigenicity

The changes in the secondary structure of PF4 observed with CD spectroscopy highly resemble the concentration dependence of PF4/UFH complex antigenicity obtained with the PF4/UFH EIA (29): (i) for low UFH concentrations, the antigenicity rises with increasing amount of UFH, (ii) at a certain concentration a maximum value is reached and (iii) a further increase in UFH concentration decreases the antigenicity of the PF4/UFH complex (24, 25).

Next we formed complexes of PF4 and various PAs in different concentrations, and assessed the structural changes of PF4 using CD spectroscopy and PF4/PA complex antigenicity by anti-PF4/heparin antibody binding using EIA. The PAs differed in their chain length (*N*) and degree of sulfation per saccharide monomer (*DS*), which enables to control the PF4/PA complex antigenicity (23–25): 1. variation of chain length: UFH (broad molecular weight distribution [large polydispersity] with average molecular weight of approximately 12 kDa), the low-molecular-weight heparin reviparin (LMWH, cut-off size approximately 5 kDa; *N*~16 saccharide monomers) and fondaparinux (pentasaccharide with a molecular weight of 1.7 kDa) and 2. variation of degree of sulfation: dextran sulfate (*DS*=2-2.3), UFH (*DS* = 1–1.2), 2-O, 3-O desulfated heparin (ODSH; *DS*=0.6-0.8), chondroitin sulfate A (chondSA; *DS*=0.4-0.5), hyaluronic acid (*DS*=0) and the polymer dextran (*DS*=0).

▶Figure 2 compares the results of the EIA and the CD spectroscopic measurements for UFH, reviparin, ODSH, chondSA, fondaparinux and dextran sulfate. In this figure, the PA concentration $c_{PA}$ (mg/ml) is divided by the PF4 tetramer concentration $c_{PF4}$ (mg/ml): $c_{rel}=c_{PA}/c_{PF4}$. Moreover, we used only the antiparallel β-sheet

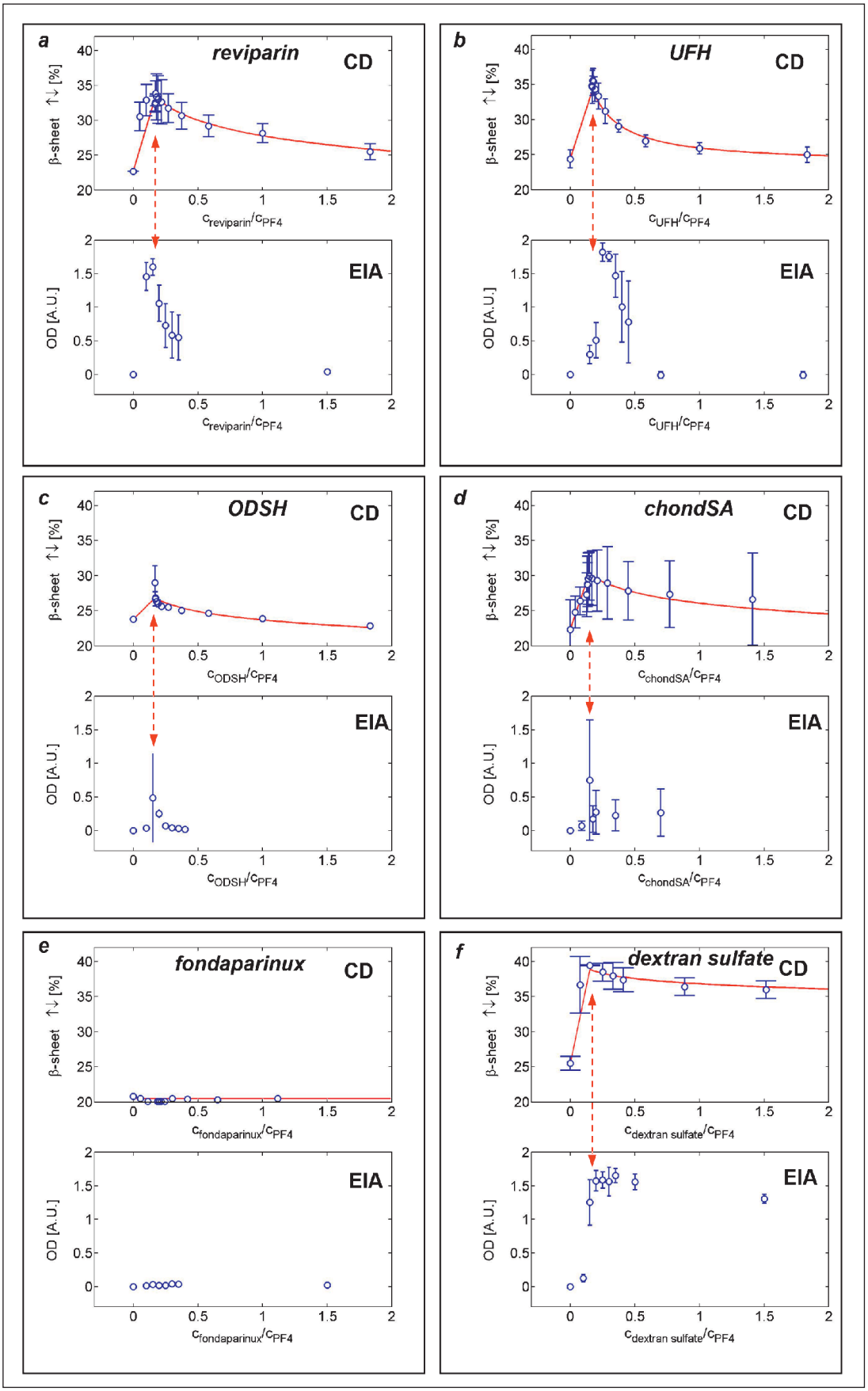


**Figure 2: Comparison of PF4 structural changes and PF4/polyanion complex antigenicity obtained from CD spectroscopic and enzyme-immunoassay (EIA) measurements.** A) Reviparin, B) unfractionated heparin (UFH), C) 2-O, 3-O desulfated heparin (ODSH), D) chondroitin sulfate A (chondSA), E) fondaparinux and F) dextran sulfate. The open circles give average values of OD (EIA) or antiparallel β-sheet content (CD spectroscopy) calculated from repetitions of these experiments, while the error bars correspond to the standard deviation (calculated from the results of n = 3 experiments using sera from 3 different patients with serologically confirmed HIT). In this figure, the PA concentration $c_{PA}$ is normalised by the PF4 tetramer concentration $c_{PF4}$: $c_{rel}=c_{PA}/c_{PF4}$. Generally, changes in PF4 secondary structure observed with CD spectroscopy are qualitatively very similar to the concentration dependence of PF4/PA complex antigenicity.

content from the CD spectroscopic measurements as an indicator since (i) it is the only type of secondary structure, which is increased during the PF4/PA interaction, and (ii) the sum of changes of all other secondary structures is balanced by this value, which makes it a suitable measure for the overall change in PF4 secondary structure.

Again, complex antigenicity (binding of anti-PF4/heparin antibodies with an OD >1) was paralleled by pronounced PF4 structural changes (antiparallel β-sheet content >30%). These changes only occurred if both, chain length *N* and *DS* (per monosaccharide unit), exceed their limiting values, which was fulfilled by UFH, reviparin, and dextran sulfate (►Figure 2A, B. F). Reviparin induced (within experimental resolution) the same maximum PF4 structural change as did UFH (antiparallel β-sheet content up to ~35%). Moreover, the maximum structural change was observed for both PAs at a relative concentration of $c_{rel}$=0.17, which corresponded to UFH or reviparin concentrations of 6.9 µg/ml at 40 µg/ml PF4.

Dextran sulfate, which has a higher degree of sulfation than UFH, induced an antiparallel β-sheet content of up to 40% (►Figure 2F), but showed no complex dissolution in excess of the PA. The PF4 secondary structure was essentially not affected by a further increase in concentration, which was indicated by almost constant values in EIA and CD spectroscopy. Among all PAs investigated, complex formation with PF4 was irreversible only for dextran sulfate.

No structural changes of PF4 were observed for fondaparinux (low *N* [23]; cf. ►Figure 2E), hyaluronic acid and dextran (low *DS* [23]; see also Suppl. Figure 1 available online at www.thrombosis-online.com).

The *DS* of ODSH and chondroitin sulfate A (chondSA) are close to the critical *DS*, as reflected in our results: we observed for both PAs an antiparallel β-sheet content of up to 30%, which is less than the values observed for the highly antigenic PAs UFH (~35%), reviparin (~35%) and dextran sulfate (~40%) but significantly larger than for native PF4 (~23.5%). Accordingly, EIA measurements show that antigenicity of PF4/ODSH and PF4/chondSA complexes is smaller in comparison to PF4/UFH, PF4/reviparin and PF4/dextran sulfate complexes, as not all but only some of the sera containing anti-PF4/PA antibodies lead to a significant OD increase. Generally, we observed striking similarities between EIA and CD spectroscopy results. This implies a close correlation between PF4/PA complex antigenicity and changes in PF4 secondary structure induced by PAs. Hence, we plotted in ►Figure 3 the OD value of PF4/PA complexes versus the PF4 antiparallel β-sheet content. For this, we directly used the data from ►Figure 2 with one exception: As we noticed for UFH a discrepancy in peak positions for OD and antiparallel β-sheet content, we introduced a correction factor of 1.75 for the UFH concentration of the CD spectroscopic data, which brings both peak positions in agreement. This reduces the horizontal scattering of the data in ►Figure 3, but does not affect the main conclusion (discussed subsequently) as can be seen in an "uncorrected version" of this figure (see Suppl. Figure 2 available online at www.thrombosis-online.com).

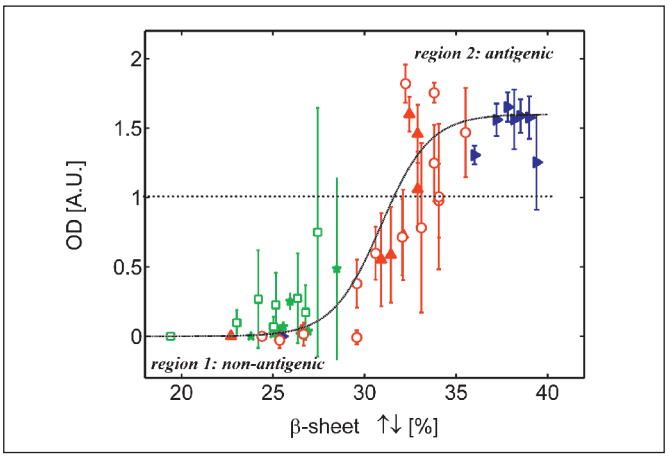


**Figure 3: PF4/PA complex antigenicity correlates with changes in PF4 antiparallel β-sheet content.** Correlation of antiparallel β-sheet content of PF4/PA complexes (as measured with CD spectroscopy) with the OD of the same complexes (as determined with EIA) for: (○) UFH, (▲) reviparin, (stars) 2-O, 3-O desulfated heparin, (□) chondroitin sulfate A, (►) dextran sulfate. Strong PF4/PA complex antigenicity (indicated by OD >> 1) is accompanied by large changes of PF4 secondary structure (indicated by antiparallel β-sheet contents >30%). As we noticed for UFH a discrepancy in peak positions for OD and antiparallel β-sheet content (see Figure 2B), we introduced a correction factor of 1.75 for the UFH concentration of the CD spectroscopic data in this plot. An "uncorrected version" of this plot is given in the supporting material. The solid line gives the fit of Eq. 1 to the data.

For an antiparallel β-sheet content smaller than 30%, the corresponding EIA gives low OD values (<<1; region 1 in ►Figure 3). An increase in antiparallel -sheet content above 30% causes a strong increase in OD (>1), which depends in first approximation linearly on the structural change (region 2 in ►Figure 3). This linear increase in OD has (within the experimental error) the same slope for all PAs.

PAs below the critical *DS* (*DS* <1) are located only in region 1, which corresponds to a small but significant change in the PF4 secondary structure without turning the PF4/PA complex antigenic. Hence, region 1 corresponds to the non-antigenic region of ►Figure 3. Additionally, as only PAs forming antigenic PF4/PA complexes are able to enter region 2 (indicated by OD values >1), this region corresponds to the antigenic region.

## Predicting PF4/PA complex antigenicity using CD spectroscopy

►Figure 3 implies a relationship between antiparallel β-sheet content and OD, which is captured by the sigmoid function (Eq. 1):

$$OD_{pred}(c_{rel}) = \frac{OD_{max}}{2} \cdot \left[1 + \tanh\left(\frac{2\Delta}{OD_{max}} \cdot \left\{\beta_{\uparrow\downarrow}(c_{rel}) - \beta_{\uparrow\downarrow,0}\right\}\right)\right]$$

Here, $c_{rel}$ denotes as before the PA concentration $c_{PA}$ (in mg/ml) normalised by the PF4 concentration $c_{PF4}$ (in mg/ml), $c_{rel}=c_{PA}/c_{PF4}$, $OD_{pred}(c_{rel})$ gives the predicted/expected OD for a complex formed at $c_{rel}$, Δ is the slope in the *antigenic region*, $\beta_{\uparrow\downarrow}(c_{rel})$ is the antipar-

allel β-sheet content at $c_{rel}$, while $\beta_{\uparrow\downarrow,0}$ sets the point of inflection of Eq. 1 and has to be determined by fitting the data to Eq. 1. $OD_{max}$ denotes the saturation OD value, which is reached for $\beta_{\uparrow\downarrow} >> \beta_{\uparrow\downarrow,0}$. This model covers both aspects discussed before, i.e. all PAs exhibit the same slope Δ and a critical structural change (here accounted by $\beta_{\uparrow\downarrow,0}$) has to be exceeded to induce a significant increase in OD. As Δ and $OD_{max}$ can be extracted from ►Figure 3, the only adjustable parameter is $\beta_{\uparrow\downarrow,0}$.

►Figure 4 compares OD values (predicted by applying Eq. 1 to CD spectroscopic data; red line and yellow area) with the ones measured by EIA (blue dots). For these calculations, we used the parameters Δ=0.3 (for β in %; taken from the slope of the linear region in ►Figure 3) and $\beta_{\uparrow\downarrow,0}$ =30.9% (fitting parameter) for all PAs. The red line corresponds to Eq. 1 applied to the average value $<\beta_{\uparrow\downarrow}>$ of the antiparallel β-sheet content $\beta_{\uparrow\downarrow}$ (as determined by CD spectroscopy; see ►Figure 2), while the yellow area accounts additionally for the fact that $\beta_{\uparrow\downarrow}$ can be resolved only within a certain measurement resolution $\Delta\beta_{\uparrow\downarrow}$(see error bars in ►Figure 2). The yellow areas correspond therefore to intervals, which are expected to contain the OD values measured by EIA.

►Figure 4 compares these OD "expectation" intervals (calculated using the CD spectroscopic data of ►Figure 2 and the average standard deviation $\Delta\beta_{\uparrow}$ =1.5%) with the results from the EIA measurements. For all PAs (except UFH), the majority of EIA data points (>85%) are located within the yellow areas, indicating that the change in antiparallel β-sheet content is converted by Eq. 1 into an indicator for complex antigenicity. However, as UFH exhibits its maximum OD at a different relative concentration $c_{rel}$ than the antiparallel β-sheet (see also ►Figure 2B), only very few EIA data points for PF4/UFH complexes hit the yellow area. If we introduce (in analogy to ►Figure 3) a correction factor for $c_{rel}$, almost all EIA data points are located in the yellow area (see Suppl. Figure 3 available online at www.thrombosis-online.com).

►Figure 4 shows that CD spectroscopy can be used to predict binding of anti-PF4/heparin antibodies to PF4/PA complexes (29). A PA can be regarded as non-antigenic if the yellow areas stay far below the threshold of OD=1.0 for all PA concentrations (►Figure 4E). It should be regarded as antigenic if the yellow area exceeds an OD of 1 (e.g. reviparin, UFH, and dextran sulfate; ►Figure 4A, B, F). In between, there might be the risk of forming weakly antigenic PF4/PA complexes, if the interval touches the antigenicity threshold (e.g. ODSH, chondroitin sulfate A; ►Figure 4C, D).

To generalise these findings, we applied CD spectroscopy to the polyphosphate polyP55 (mean chain length 55 monomers) and observed (►Figure 5) a strong increase in antiparallel β-sheet content as well as a strong increase in OD in the EIA. This shows that our approach is not restricted to PAs based on polysaccharides.

## Discussion

In this study we establish a correlation between changes in PF4 secondary structure within PF4/PA complexes with the induction of antigenic epitope(s). This approach allows to calculate expectation intervals for anti-PF4/PA antibody binding (as expressed by OD values) solely using CD spectroscopic data. In the following, we use the term antigenicity to describe that a certain PA induces a change in PF4 which results in binding of known antibodies with anti-PF4/heparin specificity to the PF4/PA complexes.

To our knowledge, this is the first demonstration that antigenicity of a drug can be assessed without the necessity of *in vivo* studies or the use of antibodies obtained from immunized patients, or special monoclonal antibodies. This approach is of potential major relevance for drug development. Several classes of biotherapeutics are negatively charged, e.g. certain anti-cancer drugs (PI-88), or DNA- or RNA-based aptamers (26, 32).

### Correlation between β-sheet formation and PF4/PA antigenicity

A critical chain length and a critical *DS* have to be exceeded by a PA to induce antigenic PF4/PA complexes: for polysaccharides, a critical chain length $N_{crit}$ of ~12 monosaccharide units and a $DS_{crit}$ of one sulfate group per saccharide monomer are frequently reported (23, 38, 39). Our measurements are in agreement with these results: non-antigenic PF4/PA complexes were formed if either the PA was too short (fondaparinux, *N*=5) or if the degree of sulfation was too low (dextran, *DS*=0; hyaluronic acid, *DS*=0.5) (23–25). For these PAs, no significant structural changes of PF4 were observed, while antigenic PF4/PA complexes were formed, if both, $N_{crit}$ and $DS_{crit}$, were simultaneously exceeded (UFH, reviparin, dextran sulfate). For these PAs, pronounced PF4 structural changes were observed.

Interestingly, among all PAs investigated only dextran sulfate showed no complex dissolution in excess of the PA (which is the usual observation for HIT-relevant PF4/PA complexes). As the main difference between dextran sulfate and the other PAs is mainly the higher (negative) line charge density, we assume that the electrostatic part of the PF4/PA-interaction is stronger for dextran sulfate than for the other PAs. However, we cannot fully rule out that also non-electrostatic effects (e.g. due to different monosaccharide conformation) might further stabilise the binding of PF4 to dextran sulfate.

The novelty here is the finding that the PF4 secondary structure can be altered by the interaction with PAs, without turning the PF4/PA complexes completely antigenic: The *DS* of ODSH and chondSA are close to the critical value of 1. These PAs induced smaller PF4 structural changes (antiparallel β-sheet content of max. 30% vs >35% for UFH) and not all sera in EIA led to a peak in OD for PF4/ODSH and PF4/chondSA complexes. Indeed, Joglekar et al. (40) showed that ODSH creates a very small risk of inducing immune reactions to PF4/ODSH complexes. Our interpretation of the more variable binding of the anti-PF4/PA antibodies to the complexes between PF4 and ODSH or chondroitin sulfate is that the epitope is expressed in a suboptimal way on the PF4/ODSH and PF4/chondroitin sulfate complexes, respectively. This indicates that the antibodies we used differ slightly, either in the binding sites they recognise on PF4 or in their affinity. Antibodies showing high affinity may still bind despite a less optimal

 

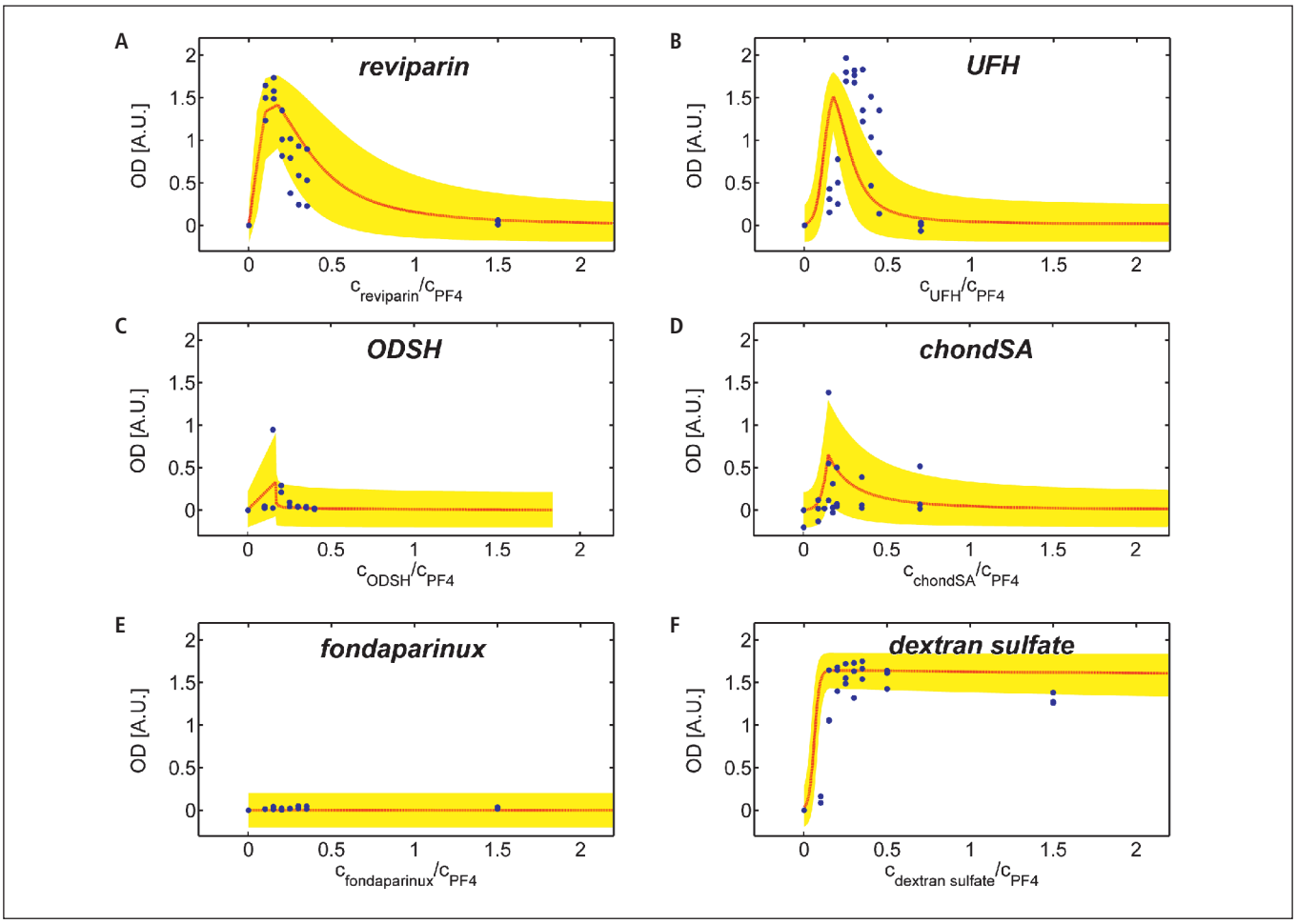


**Figure 4: CD spectroscopy allows prediction of PA concentration dependent PF4/PA complex antigenicity.** Comparison of OD values predicted from the CD spectroscopic measurements (red line and yellow areas) with the ones measured by EIA (blue dots). The red line is calculated according to Eq. 1 and translates the average value of PF4 antiparallel β-sheet content (see symbols in Figure 2) into an OD value of the PF4/PA complex in EIA measurements. The yellow areas are calculated in a similar way, but additionally account for measurement uncertainties in the determination of the secondary structure (see error bars in Figure 2). This means that from Eq. 1 (which is based on the correlation observed in Figure 3) we expect the data points of EIA measurements on PF4/PA complexes to be located within the yellow areas, which is indeed fulfilled for all PAs investigated (except UFH, see text for discussion). This shows that the antiparallel β-sheet content is quantitatively connected with the antigenicity of a PF4/PA complex. Moreover, results of EIA measurements can be predicted from CD spectroscopic measurements, i.e. CD spectroscopy in connection with Eq. 1 can be used to assess antigenicity of PF4/PA complexes.

expression of the conformation dependent neoepitope induced by the PA.

For all PAs tested we observed that the increase in antiparallel β-sheet content is balanced by a decrease in structures having α-helical or β-turn conformations. This suggests that the antiparallel β-sheet content might be indicative for the antigenicity of the PF4/PA complex, which was confirmed by correlating EIA and CD spectroscopic data.

Using these considerations it was possible to predict PF4/PA complex antigenicity solely from the antiparallel β-sheet content (as measured by CD spectroscopy; ▶Figure 4). As the peak PA concentrations of both approaches coincide in all (except one) cases, we conclude that maximum antigenicity is obtained at a PA concentration that also induces maximum change in PF4 antiparallel β-sheet content. Exposure of HIT-relevant epitope(s) is only observed for PAs that also change the secondary structure of PF4. Hence, it is not sufficient to form a repetitive PF4 alignment on the PA chain, as we hypothesised in previous studies (16).

One might argue, whether the differences in the antibody binding capacity for the different PAs might be caused by the charge and/or length of the respective PA. We are relatively confident that the charge does not inhibit the access of an IgG to the epitopes, as complexes of PF4 with dextran sulfate and hypersulfated chondroitin sulfate show even better antibody binding than UFH (23). The length of the PA has an indirect impact on antibody binding as a certain chain length $N_{crit}$ has to be exceeded to induce antigenic PF4/PA-complexes. The existence of $N_{crit}$ led to the hypothesis that at least two PF4 tetramers have to be connected by one PA

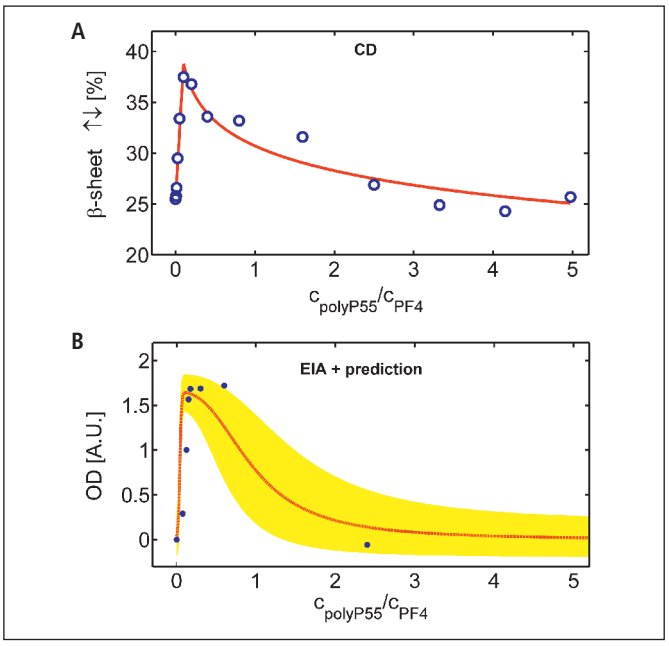


**Figure 5: Polyphosphates form antigenic complexes with PF4.** Comparison of PF4 structural changes and PF4/polyP55 antigenicity obtained from A) CD spectroscopic and B) EIA measurements. Similar to the PAs of Figure 2, one observes that changes in PF4 secondary structure (indicated by a strong increase in antiparallel β-sheet content; open circles in A) are accompanied by complex antigenicity (indicated by OD values far exceeding 1; dots in B). Moreover, B) compares OD values predicted from the CD spectroscopic measurements (red line and yellow area) with the ones measured by EIA (blue dots) for PF4/polyP55 complexes (see caption of Figure 4 and text for details). Again, the data points of the EIA measurements are mostly located within the expected (yellow) area, which shows that results of EIA measurements can be predicted from CD spectroscopy (using Eq. 1) also for PAs carrying phosphate groups.

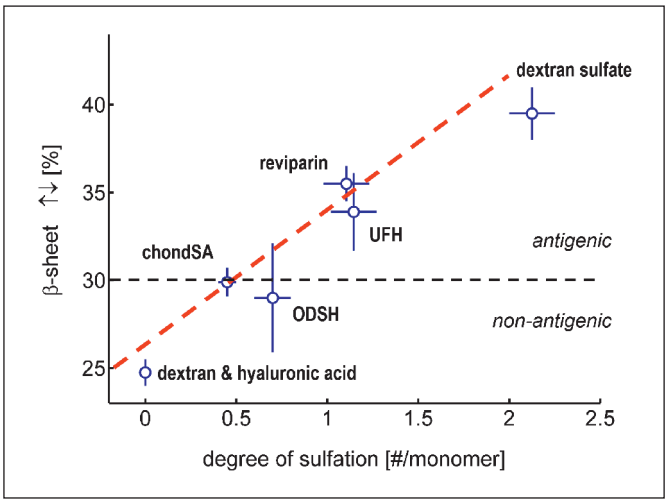


**Figure 6: Maximum change in PF4 secondary structure correlates with the polyanion's degree of sulfation.** Relation between degree of sulfation, *DS*, and maximum change in antiparallel β-sheet content for PF4/PA complexes as indicated. An almost linear increase in maximum structural change is observed.

chain to make the formed complex antigenic (16). Depending on the PA's *N* and *DS*, each PF4 tetramer occupies a certain amount of monomers on the PA chain, which limits the maximum number of PF4 tetramers that can be bound to a PA chain. However, a single chain must be able to bind at least two PF4 tetramers to induce epitope expression and antibody binding. That very long PAs (having the capability to bind many PF4 tetramers) do not mediate antibody binding to PF4 is likely not caused by charge related hindrance of antibody binding, but, as we have shown by systematic studies many years ago (25), this is more likely caused by wrapping of the PA around PF4 instead of bridging between PF4 molecules. As the PAs bind to the equatorial ring of positively charged amino acids, it should be sufficiently far away from the antibody binding site. Thus the length of the polyanion likely does not interfere with IgG binding, but influences it indirectly via saturation of all binding sites of PF4 which prevents formation of multimolecular complexes. These complexes seem to be essential for antigenicity and even the conformational changes in PF4 seem to be influenced by complex formation of several PF4 molecules.

This reasoning can be generalized to show that the changes in antibody binding of the different PF4/PA-complexes cannot be caused by steric or electrostatic inhibition of antibody access. A steric hindrance would be largest in the presence of highly charged PAs. Hence, in this case PF4/dextran sulfate- and PF4/polyP55-complexes should have the lowest antibody binding capacity, which is also not observed in the experiment. Therefore, we rule out that biophysical features of the PAs affect antibody access sterically or electrostatically unless a certain length is not exceeded. Our data rather show that PA binding to PF4 creates (a) new epitope(s) by inducing a change in PF4 secondary structure. These neoepitopes are likely also dependent on the close approximation of several PF4 tetramers. However, the latter is still speculative.

Up to now, we found deviations between CD spectroscopy and EIA only for UFH, while for the LMWH reviparin (which is chemically equivalent to UFH but exhibits a much narrower size distribution) a good agreement was obtained. As the chain length distribution of UFH is much broader with respect to the other PAs, we hypothesise that the discrepancy of the peak positions in CD spectroscopy and EIA are caused by the polydispersity of UFH.

It is evident from ▶Figure 4 that the data from the CD spectroscopy can be used to predict whether a PA has a high likelihood to induce the binding sites for anti-PF4/PA antibodies for all less polydisperse PAs and hence, to get a measure for the PF4/PA complex antigenicity solely from CD spectroscopic measurements. The antigenicity threshold is reached at an antiparallel β-sheet content of approximately 30%, i.e. PAs inducing PF4 structural changes that exceed that threshold constitute antigenic PF4/PA complexes. A similar value is obtained if the dependence between degree of sulfation *DS* and maximum value of PF4 antiparallel β-sheet content is plotted for all PF4/PA complexes investigated and one regards that PF4/ODSH and PF4/chondSA complexes are at the antigenic threshold (▶Figure 6).

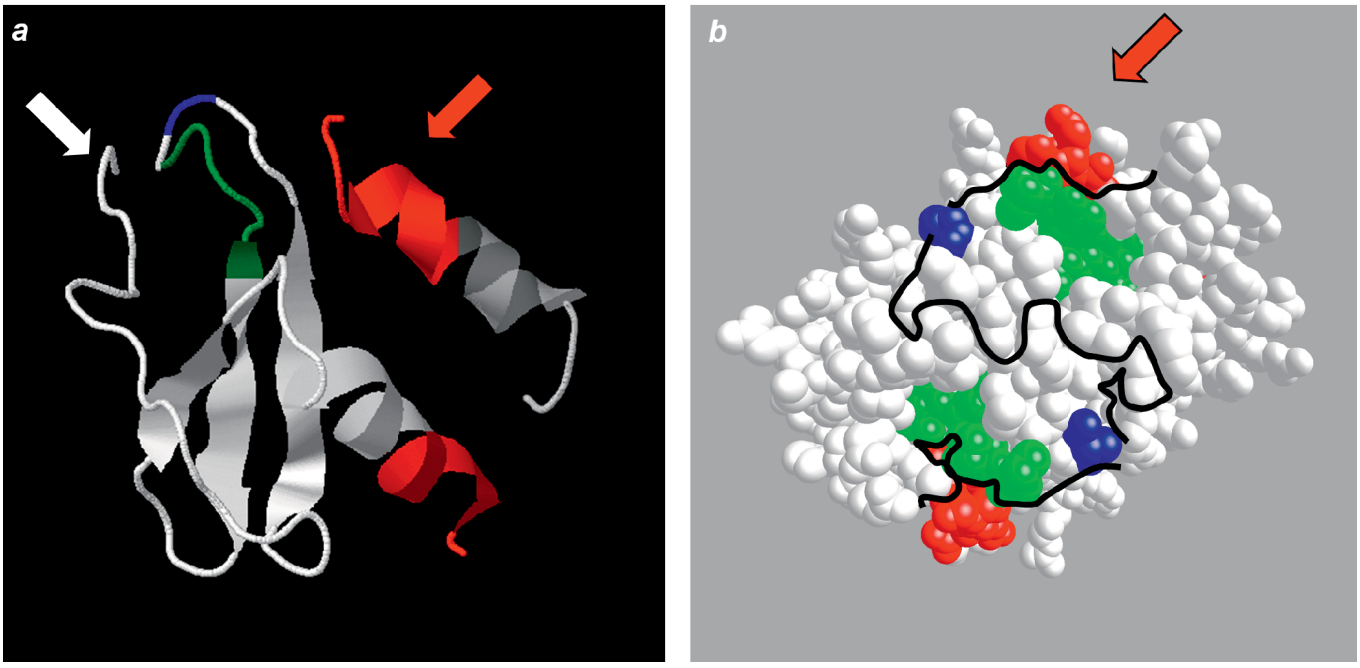


**Figure 7: Structural model for the conformational changes of PF4 induced by PF4/polyanion complex formation.** Molecular model of a) the secondary structure of a PF4 monomer (supplemented by the α-helix of the adjacent PF4 monomer) and b) the surface of a PF4 tetramer as determined by X-ray crystallographic measurements of Zhang et al. (46) (code 1RHP of the Brookhaven Protein Data Bank). The three curved, black lines in b) indicate the course of the interfaces between the four PF4 monomers that together form the homotetramer. The view axis in b) is perpendicular to the plane of the PF4 heparin binding site and shows that the majority of the amino acids (constituting the protein surface) belong to solely two monomers above the heparin binding side (while the remaining two monomers form the majority of the surface on the opposite side). The two known HIT related epitopes (site 1 = amino acids 37–41: green structures; amino acid 34 belongs to site 2: blue structures) are located at a β-turn hairpin. Both epitopes are neighboured by the C-terminal amino acids (amino acids 66–70: red arrow) and red structures in b) of the α-helix of the adjacent PF4 monomer (with respect to the plane defined by the heparin binding site) so that the epitopes and the C-terminal part of the α-helix form a continuous patch on the surface of the PF4 tetramer. Due to this interplay between neighboured PF4 monomers, this patch is only exposed if PF4 is in a tetrameric form.

While findings of *in vitro* experiments are largely compatible with our model, there is, however, a conflicting clinical observation in regard to fondaparinux. Patients receiving fondaparinux after major orthopaedic surgery developed anti-PF4/heparin antibodies (41). On the other hand, patients with acute HIT can be treated safely with fondaparinux. A potential explanation (42) might be that other polyanions, like heparan sulfate act together with fondaparinux as a feeder for PF4-complex formation (43) in large enough quantities for immunisation but in too low concentrations for inducing immune-complex mediated activation of platelets. This puzzling issue requires further investigations.

The almost complete lack of cross-reactivity of anti-PF4/heparin antibodies against PF4/danaparoid complexes is also compatible with our findings. First of all, danaparoid is mostly (>95%) a mixture of GAGs, whose degree of sulfation *DS* is generally smaller than the critical $DS_{crit} \sim 1$, which already indicates that (similar to ODSH and chondroitin sulfate A, chondSA) at most a very weak cross-reactivity is expected. Nevertheless, danaparoid also has a small content of highly sulfated heparin, which contributes to about 5% of the drug. This constituent of danaparoid with high affinity to antithrombin fully reacts with anti-PF4/heparin antibodies (44). However, due to the relatively low specific activity of danaparoid much more danaparoid is given on a weight basis. While low molecular weight heparin has an anti-FXa activity of ~100 U/mg, the activity of danaparoid is only 15 U/mg. Both drugs are dosed according to the anti-FXa plasma levels, which are in therapeutic dose about 0.4 – 0.6 anti-FXaU/ml for danaparoid given as continues infusion. Thus on a molecular basis there are about 6–7 times more PA molecules administered. We have shown that the mixture of 5% high antithrombin affinity drug plus 95% low antithrombin affinity material completely blocks platelet activation by HIT antibodies, which has more recently been further characterised by our group (44, 45).

Another issue, however, can be explained more easily. In some patients, typically suffering from severe HIT, it was observed that their sera contain antibodies that directly bind to PF4 (i.e. complex formation with polyanions like heparin is not necessary for these sera). As these antibodies bind to PF4 also in absence of polyanions, it is very likely that they recognise epitopes on PF4 that are not dependent on conformational changes of PF4. We can only speculate that these antibodies are created in parallel during the immune response against the PF4/heparin-complexes. Typically these antibodies, which react with PF4 in the absence of heparin, are present in sera showing a very high OD in the antigen assays

### What is known about this topic?

- Platelet factor 4 (PF4) and polyanions like heparin form complexes. Some of these complexes are antigenic, i.e. they react with anti-PF4/heparin antibodies.
- Only PF4 tetramers can expose the antigen to which anti-PF4/heparin antibodies bind.
- It is unclear whether the epitope to which anti-PF4/heparin antibodies bind results from a conformational change of PF4 or from close approximation of two PF4 tetramers.
- Platelets contain polyphosphates in their dense granules

### What does this paper add?

- The described method is the first to screen new drugs for their potential immunogenicity by inducing a conformational change in PF4.
- To the best of our knowledge this is the first report describing how a complex neoantigen is expressed on an endogenous protein resulting from a conformational change AND formation of densely packed proteins. This may serve as a model to better understand formation of autoantigens.
- It shows that the epitope recognised by HIT antibodies is induced by a change in the conformation of PF4 which requires both, binding of the polyanion and close approximation of two PF4 molecules, hereby combining two of the currently discussed models.
- Characterisation of the antigenic epitope as a composite epitope of the β-strands of one PF4-monomer and the α-helix of the adjacent monomer. This is the explanation for the long known empirical observation that only PF4 tetramers are able to expose the HIT antigen.
- The described method of CD spectroscopy can be used by all manufacturers of HIT antibody assays as an in-process quality control to identify optimal and/or false lots of PF4/heparin complexes.
- Polyphosphates interact strongly with PF4 and induce a conformational change in PF4.

and show very strong platelet activation in the functional assays. A similar mechanism is observed in post transfusion purpura, in which boosting of an immune response to the human platelet antigen (HPA)-1a results in formation of antibodies, which also bind to the HPA-1a negative autologous platelets of the patient (i.e. they behave like autoantibodies), causing severe thrombocytopenia. Also these sera react very strongly against the platelet glycoprotein IIbIIIa in EIAs. Whether this is the well-known phenomenon of epitope spreading during the acute phase of B-cell stimulation or whether there is another underlying cause is currently unresolved.

## Model of PF4 structural changes based on the CD spectroscopic data

X-ray diffraction studies performed on bovine and human PF4 showed that the PF4 monomer consists of a single α-helix (located at the C-terminus; amino acids (AA) 60–70), which is followed by three antiparallel β-sheet strands (AA 24–31, 39–44 and 49–53) (35, 46). Four β-turn structures connect the three β-sheet strands and the α-helix (►Figure 7A). The remaining part of PF4 (AA 1–19) adopts an unordered conformation.

As the axes of the α-helix and the β-sheet strands enclose an angle of approximately 45°, this configuration belongs to *class 2* in the nomenclature of Chou et al. (35, 47). The α-helix contains a cluster of four lysines, which are known to be a prerequisite for PF4 binding to heparin or other PAs. In its tetrameric form, the four α-helices and most of the positively charged AAs form a positively charged "ring" around the PF4 tetramer, which is expected to be the actual heparin binding site (46).

By analysing the binding capacity of anti-PF4/UFH antibodies to complexes made of UFH and mutations of PF4, the group of Dr. Poncz in Philadelphia located two different HIT-related epitopes (48, 49). Site-1 is located between the PF4 AAs 37–41, which are part of a β-turn hairpin structure connecting β-sheet strand 1 and 2 (green structures in ►Figure 7). This site is recognised by sera of approximately one third of PF4/PA antibodies (48). Site-2 involves the N-terminus (white arrow in ►Figure 7A) and at least AA 34 (blue structures in ►Figure 7) and is recognised by KKO, a HIT-like monoclonal antibody (50). Recently, it was shown that only those anti-PF4/UFH antibodies activate platelets which compete with KKO (51). This shows that site-2 constitutes or at least overlaps with an area that is recognised by a large fraction of anti-PF4/UFH antibodies and has therefore high clinical relevance (49). Interestingly, it seems that the C-terminal part of PF4 (AA 44–70) is not related to any epitope, as they are not recognised by anti-PF4/UFH antibodies (52) and as antibodies specific to these AAs do not compete with binding of anti-PF4/UFH antibodies to the PF4/UFH complex (48).

CD spectroscopy suggests that AAs adopting a β-turn or a α-helical secondary structure are transformed into an antiparallel β-sheet. As the anti-PF4/heparin antibody binding site-1 (AA 37–41) and parts of site-2 (AA 34) are directly located at the β-turn hairpin (AA 32–38), it is very likely that the structural changes occur in the vicinity of these sites. This is further supported by the length of the β-turns: Only the β-turn hairpin (AA 32–38) is long enough to allow a (partly) transition to antiparallel β-sheets, while the other β-turns are much shorter (making this transition rather unlikely).

The observation that epitope formation is accompanied by a structural change of the α-helix was unexpected as (i) it is currently believed that the C-terminal amino acids are not involved in HIT-related epitope formation (48, 52), and (ii) as the α-helix is located oppositely to the yet known epitopes in the PF4 monomer. However, modelling the PF4 dimer (as done by Zhang et al. [46]) indicates that the C-terminal AAs of the α-helix of one PF4 monomer (red arrow and red structures in ►Figure 7) are close to

site-1 and -2 of the adjacent PF4 monomer (green and blue structures in ▶Figure 7). Hence, although there is a large distance between the α-helix and the known epitopes within a single PF4 monomer, these structures become closely placed in the PF4 dimer and tetramer.

This suggests that structural changes of the α-helix create (a) new epitope(s) which are directly neighboured to the known epitope(s) site-1 and -2, forming a large antigenic patch at the surface of PF4 (▶Figure 7B). AAs 66–70 are involved in the expression of the epitope. These AAs are part of the α-helix of the native PF4, and neighbour the known epitopes on the PF4 surface. Therefore it is likely that they are part of the epitope. This interplay between antigenic structures of neighboured PF4 monomers explains the observation that the ability to form antigenic PF4/UFH complexes depends strongly on the ability of PF4 to form tetramers: complexes made of UFH and non-tetrameric PF4 (i.e. PF4 that is unable to form tetramers) showed a much lower antigenicity with respect to tetrameric PF4 (43). Hence, in its tetrameric form PF4 exposes four antigenic patches (two on each side of the plane defined by the heparin binding site), making these patches highly available for antibody binding regardless of the actual PF4 orientation within the PF4/PA complex.

### Study limitations

Although the correlation between EIA and CD spectroscopy looks very promising, there are some limitations resulting from approximations done in this study. First of all, to measure antigenicity we used sera from three different patients only, which probably do not represent the full reactivity pattern of all anti-PF4/heparin antibodies. Moreover, we are aware that EIA typically does not exhibit a linear dependence from the amount of bound antibodies and that we cannot assume steady state binding of clinically-relevant anti-PF4/heparin antibodies from patient sera to PF4/PA-complexes, making a quantitative interpretation of the OD in terms of antigenicity challenging.

However, even using this relatively easy to apply "crude" approach, we get very reproducible results with various PAs. This strongly indicates that the system is stable and allows a robust assessment. Otherwise one would expect variable results, a wide range of reactivities and no clear correlation between the peak signals in the EIA and the CD spectroscopy at the same PA concentrations. Increasing the numbers of sera (for future experiments) and resolving the functional dependence between antibody binding capacity and OD in EIA might enhance the accuracy of the correlation and allow for even more precise *in vitro* assessment of PA antigenicity.

### Conclusion

CD spectroscopy is found to be a powerful technique to monitor structural changes of PF4 caused by binding to various polyanions (PA). In all cases, exposure of HIT-relevant epitope(s) is only observed for PAs that also induce changes in PF4 secondary structure. A comparison of results of an immunoassay with CD spectroscopic data showed that the extent of complex antigenicity correlates well with the magnitude of changes in PF4 secondary structure, and that a minimum structural change of PF4 is necessary to achieve PF4/PA complex antigenicity. These findings allowed us to calculate expectation intervals for complex antigenicity solely using CD spectroscopic data. To our knowledge, this is the first demonstration that the capability of drugs to induce antigenicity of PF4 can be assessed without the necessity of *in vivo* studies or the use of antibodies obtained from immunised patients specific for the antigens. Although shown only for PF4, our finding might be applicable to other proteins that also express epitopes upon changes in their secondary structure. This will be addressed in future studies.

## Supplementary Material

In the Supplementary Material, which is available online at www.thrombosis-online.com, results of CD spectroscopic measurements on PF4/dextran and PF4/hyaluronic acid complexes are given. Moreover, versions of Figures 3 and 4B are supplied, which use no correction factor for the UFH data.

**Acknowledgement**

S. Brandt, K. Krauel and S. Block were supported by the "Zentrum für Innovationskompetenz Humorale Immunreaktionen bei Kardiovaskulären Erkrankungen" (ZIK HIKE, Federal Ministry of Education and Research-BMBF FKZ 03Z2CN11 and FKZ 03Z2CN12). S. Block also acknowledges support by the European Social Fund (grant number UG 10 022). T. Renné acknowledges funding by Vetenskapsrådet (K2013–65X-21462–04–5), and the ERC StG-2012–311575.

**Conflicts of interest**

None declared.

## References

1. Schellekens H. The immunogenicity of therapeutic proteins. Discov Med 2010; 49: 560–564.
2. Schellekens H. Bioequivalence and the immunogenicity of biopharmaceuticals. Nat Rev Drug Discov 2002; 1: 457–462.
3. Moreland LW, McCabe DP, Caldwell JR, et al. 3rd. Phase I/II trial of recombinant methionyl human tumor necrosis factor binding protein PEGylated dimer in patients with active refractory rheumatoid arthritis. J Rheumatol 2000; 27: 601–609.
4. Rau R, Sander O, van Riel P, et al. Intravenous human recombinant tumor necrosis factor receptor p55-Fc IgG1 fusion protein Ro 45–2081 (lenercept): a double blind, placebo controlled dose-finding study in rheumatoid arthritis. J Rheumatol 2003; 30: 680–690.
5. Eichler P, Lubenow N, Strobel U, et al. Antibodies against lepirudin are polyspecific and recognize epitopes on bivalirudin. Blood 2004; 103: 613–616.
6. Greinacher A, Lubenow N, Eichler P. Anaphylactic and anaphylactoid reactions associated with lepirudin in patients with heparin-induced thrombocytopenia. Circulation 2003; 108: 2062–2065.

7. Casadevall N, Nataf J, Viron B, et al. Pure red-cell aplasia and antierythropoietin antibodies in patients treated with recombinant erythropoietin. N Engl J Med 2002; 346: 469–475.
8. van Beers MMC, Sauerborn M, Gilli F, et al. Aggregated recombinant human interferon beta induces antibodies but no memory in immune tolerant transgenic mice. *Pharm Res* 2010; 27: 1812–1824.
9. Hemmer B, Stüve O, Kieseier B, et al. Immune response to immunotherapy: the role of neutralising antibodies to interferon beta in the treatment of multiple sclerosis. Lancet Neurol 2005; 4: 403–412.
10. Arepally GM, Ortel TL. Clinical practice. Heparin-induced thrombocytopenia. N Engl J Med 2006; 355: 809–817.
11. Wolpe SD, Cerami A. Macrophage inflammatory protein-1 and protein-2 – members of a novel superfamily of cytokines. Faseb J 1989; 3: 2565–2573.
12. Huang SS, Huang JS, Deuel TF. Proteoglycan carrier of human-platelet factor-4 – isolation and characterisation. J Biol Chem 1982; 257: 1546–1550.
13. Kaplan KL, Broekman MJ, Chernoff A, et al. Platelet alpha-granule proteins: studies on release and subcellular localisation. Blood 1979; 53: 604–618.
14. Rucinski B, Niewiarowski S, James P, et al. Antiheparin proteins secreted by human platelets. purification, characterisation, and radioimmunoassay. Blood 1979; 53: 47–62.
15. Deuel TF, Keim PS, Farmer M, et al. Amino-acid sequence of human platelet factor 4. PNAS 1977; 74: 2256–2258.
16. Greinacher A, Gopinadhan M, Günther J-U, et al. Close approximation of two platelet factor 4 tetramers by charge neutralisation forms the antigens recognized by HIT antibodies. Arterioscl Thromb Vasc Biol 2006; 26: 2386-2393.
17. Rauova L, Poncz M, McKenzie SE, et al. Ultralarge complexes of PF4 and heparin are central to the pathogenesis of heparin-induced thrombocytopenia. Blood 2005; 105: 131–138.
18. Chong BH, Pitney WR, Castaldi PA. Heparin-induced thrombocytopenia – association of thrombotic complications with heparin-dependent Igg antibody that induces thromboxane synthesis and platelet-aggregation. Lancet 1982; 2: 1246–1249.
19. Amiral J, Bridey F, Dreyfus M, et al. Platelet factor-iv complexed to heparin is the target for antibodies generated in heparin-induced thrombocytopenia. Thromb Haemost 1992; 68: 95–96.
20. Warkentin TE, Greinacher A. Heparin-induced thrombocytopenia: recognition, treatment, and prevention. Chest 2004; 126: 311s-337s.
21. Cines D, Kaywin P, Bina M, et al. Heparin associated thrombocytopenia. N Engl J Med 1980; 303: 788–795.
22. Chong BH, Fawaz I, Chesterman CN, et al. Heparin induced thrombocytopenia: mechanism of interaction of the heparin dependent antibody with platelets. Br J Haematol 1989; 73: 235–240.
23. Alban S, Krauel K, Greinacher A. Role of Sulfated Polysaccharides in the Pathogenesis of Heparin-Induced Thrombocytopenia. In: Heparin-Induced-Thrombocytopenia (Fundamental and Clinical Cardiology), 5th edition. LLC: Boca Raton, USA: Taylor and Francis Group; 2013: pp. 181–208.
24. Kelton JG, Smith JW, Warkentin TE, et al. Immunoglobulin-G from Patients with Heparin-Induced Thrombocytopenia Binds to a Complex of Heparin and Platelet Factor-4. Blood 1994; 83: 3232–3239.
25. Greinacher A, Alban S, Dummel V, et al. Characterisation of the structural requirements for a carbohydrate based anticoagulant with reduced risk of inducing the immunological type of heparin-associated thrombocytopenia. Thromb Haemost 1995; 74: 886-892.
26. Jaax ME, Krauel K, Marschall T, et al. Complex formation with nucleic acids and aptamers alters antigenic properties of platelet factor 4. Blood 2013; 122: 272-281.
27. Mikhailov D, Young HC, Linhardt RJ, et al. Heparin dodecasaccharide binding to platelet factor-4 and growth-related protein-alpha. J Biol Chem 1999; 274: 25317–25329.
28. Bohm G, Muhr R, Jaenicke R. Quantitative-analysis of protein far UV circular-dichroism spectra by neural networks. Protein Engin 1992; 5: 191–195.
29. Juhl D, Eichler P, Lubenow N, et al. Incidence and clinical significance of anti-PF4/heparin antibodies of the IgG, IgM, and IgA class in 755 consecutive patient samples referred for diagnostic testing for heparin-induced thrombocytopenia. Eur J Haematol 2006; 76: 420–426.
30. Sreerama N, Woody RW. Computation and Analysis of Protein Circular Dichroism Spectra. In: Methods in Enzymology 383. San Diego, CA: Elsevier Academic Press; 2004: pp. 318–351.
31. Krauel K, Pötschke C, Weber C, et al. Platelet factor 4 binds to bacteria-inducing antibodies cross-reacting with the major antigen in heparin-induced thrombocytopenia. Blood 2011; 117: 1370–1378.
32. Rosenthal MA, Rischin D, McArthur G, et al. Treatment with the novel anti-angiogenic agent PI-88 is associated with immune-mediated thrombocytopenia. Ann Oncol 2002; 13: 770–776.
33. Mayo KH, Barker S, Kuranda MJ, et al. Molten globule monomer to condensed dimer – role of disulfide bonds in platelet factor-iv folding and subunit association. Biochemistry 1992; 31: 12255–12265.
34. Villanueva GB, Allen N, Walz D. Circular-dichroism of platelet factor-4. Arch Biochem Biophys 1988; 261: 170–174.
35. Charles RS, Walz DA, Edwards BFP. The 3-dimensional structure of bovine platelet factor-4 at 3.0-A resolution. J Biol Chem 1989; 264: 2092-2099.
36. Gans PJ, Lyu PC, Manning MC, et al. The helix-coil transition in heterogeneous peptides with specific side-chain interactions: theory and comparison with CD spectral data. Biopolymers 1991; 31: 1605–1614.
37. Chin D-H, Woody RW, Rohl CA, et al. Circular dichroism spectra of short, fixed-nucleus alanine helices. PNAS 2002; 99: 15416–15421.
38. Leroux D, Canépa S, Viskov C, et al. Binding of heparin-dependent antibodies to PF4 modified by enoxaparin oligosaccharides: evaluation by surface plasmon resonance and serotonin release assay. J Thromb Haemost 2012; 10: 430–436.
39. Petitou M, Hérault JP, Bernat A, et al. Synthesis of thrombin-inhibiting heparin mimetics without side effects. Nature 1999; 398: 417–422.
40. Joglekar MV, Quintana Diez PM, Marcus S, et al. Disruption of PF4/H multimolecular complex formation with a minimally anticoagulant heparin (ODSH). Thromb Haemost 2012; 107: 717–725.
41. Warkentin TE, Cook RJ, Marder VJ, et al. Anti-platelet factor 4/heparin antibodies in orthopedic surgery patients receiving antithrombotic prophylaxis with fondaparinux or enoxaparin. Blood 2005; 106: 3791–3796.
42. Warkentin TE, Pai M, Sheppard JI, et al. Fondaparinux treatment of acute heparin-induced thrombocytopenia confirmed by the serotonin-release assay: a 30-month, 16-patient case series. J Thromb Haemost 2011; 9: 2389–2396.
43. Sachais BS, Litvinov RI, Yarovoi SV, et al. Dynamic antibody-binding properties in the pathogenesis of HIT. Blood 2012; 120: 1137–1142.
44. Greinacher A, Michels I, Mueller-Eckhardt C. Heparin-associated thrombocytopenia: the antibody is not heparin specific. Thromb Haemost 1992; 67: 545–549.
45. Krauel K, Fürll B, Warkentin TE, et al. Heparin-induced thrombocytopenia–therapeutic concentrations of danaparoid, unlike fondaparinux and direct thrombin inhibitors, inhibit formation of platelet factor 4–heparin complexes. J Thromb Haemost 2008; 6: 2160–2167.
46. Zhang X, Chen L, Bancroft DP. Crystal-structure of recombinant human platelet factor-4. Biochemistry 1994; 33: 8361–8366.
47. Chou K-C, Nemethy G, Rumsey S, et al. Interactions between an alpha-helix and a beta-sheet energetics of alpha-beta-packing in proteins. J Mol Bio 1985; 186: 591–609.
48. Ziporen L, Li ZQ, Park KS, et al. Defining an antigenic epitope on platelet factor 4 associated with heparin-induced thrombocytopenia. Blood 1998; 92: 3250–3259.
49. Li ZQ, Liu W, Park KS, et al. Defining a second epitope for heparin-induced thrombocytopenia/thrombosis antibodies using KKO, a murine HIT-like monoclonal antibody. Blood 2002; 99: 1230–1236.
50. Arepally GM, Park KS, Kamei S, et al. Characterisation of a murine monoclonal antibody that mimics heparin-induced thrombocytopenia antibodies. Blood 2000; 95: 1533–1540.
51. Cuker A, Rux AH, Hinds JL, et al. Novel diagnostic assays for heparin-induced thrombocytopenia. Blood 2012; 120: 267.
52. Suh JS, Aster RH, Visentin GP. Antibodies from patients with heparin-induced thrombocytopenia/thrombosis recognize different epitopes on heparin: platelet factor 4. Blood 1998; 91: 916–922.


 